Arabian Journal of Geosciences (2019) 12: 62
https://doi.org/10.1007/s12517-018-4217-8

ORIGINAL PAPER

Geoelectrical parameters for the estimation of hydrogeological properties

M. T. Noorellimia [1] · W. Aimrun [1,2] · M. M. Z. Azwan [1,2] · A. F. Abdullah [1,2]

Received: 25 August 2017 / Accepted: 28 December 2018 / Published online: 15 January 2019

Abstract
Excessive groundwater extraction could cause environmental degradation such as surface water depletion, saltwater intrusion, and many more. Therefore, groundwater should be extracted in sustainable way to avert the harmful consequences. An accurate amount of sustainable groundwater yield can be obtained through the groundwater flow model that has low uncertainty. It is important to incorporate the actual hydrogeological properties into groundwater flow modeling to reduce the uncertainty. The purpose of this study is to estimate hydrogeological properties, namely, hydraulic conductivity (K) and transmissivity (T), by combining the electrical resistivity (ER) and induced polarization (IP) methods into an analytical equation. This study used an analytical equation that relates the geoelectrical parameters to the hydrogeological properties. The ER and IP methods were applied to improve the accuracy of geoelectrical parameters using the ABEM Lund Imaging system. The developed analytical equation was compared with other studies for verification. The results showed that the analytical equation model developed in this study had the lowest error compared to that of other published analytical equation models. Therefore, the combination of the ER and IP methods with a new proposed constant value for the analytical equation increased the accuracy of hydrogeological properties.

Keywords Hydraulic conductivity · Transmissivity · Analytical equation · Geoelectrical imaging survey · Induced polarization · Electrical resistivity

Introduction

Generally, groundwater flow modeling is used to estimate the sustainable groundwater yield. However, groundwater flow modeling is commonly associated with high uncertainty, mostly resulting from uncertainty in the hydrogeological properties, such as K and T. Traditionally, hydrogeological properties have been obtained by analyzing pumping test data. However, installation of a tube well and the pumping test activity are costly. Therefore, the hydrogeological properties for several locations within the study area are unattainable using a pumping test.

Hydrogeological properties are theoretically based on the subsurface geological formation's porosity. The electrical properties of the geological formation are also correlated with the porosity (petrophysical property). Based on their mutual dependence on porosity, the hydrogeological properties can be correlated with the electrical properties (Slater 2007). The regression equation can be made by comparing the hydrogeological properties from a pumping test and the hydrogeological properties derived from geoelectrical parameters (Dar-Zarrouk parameters) (Batte et al. 2010; Perdomo et al. 2014; Taheri et al. 2007). The simple regression can predict K with approximately 60–90% confidence (Farid

✉ M. T. Noorellimia
noorellimia1@gmail.com

[1] Department of Biological and Agricultural Engineering, Faculty of Engineering, Universiti Putra Malaysia (UPM), 43400 Serdang, Selangor, Malaysia

[2] SMART Farming Technology Research Centre, Faculty of Engineering, Universiti Putra Malaysia (UPM), 43400 Serdang, Selangor, Malaysia

et al. 2013). A high regression coefficient indicates that the hydrogeological properties derived from geoelectrical parameters are similar to the hydrogeological properties obtained from the pumping test.

There have been many studies targeted at improving the regression equation. It was found that the relationship between the hydrogeological properties and the geoelectrical parameters depends on the degree of saturation (Khalil and Monterio Santos 2009). For the increment in the regression coefficient, Batayneh (2009) suggested accounting for different hydraulic units, while Sinha et al. (2009) suggested adding several geoelectrical parameters. However, for the regression equation, several pumping tests must be conducted in order to obtain the hydrogeological properties. According to Mastrocicco et al. (2009), at least five pumping tests should be performed to develop the regression equation; this testing is expensive and time taking. Alternatively, Soupios et al. (2007) obtained the hydrogeological properties from the Archie equation rather than a pumping test (Utom et al. 2013). The Archie equation is used to estimate the porosity, and then, K is obtained from the Kozeny-Carmen equation. However, the method is not applicable to a hard rock aquifer.

In addition to the regression equation, an analytical equation can also be used to estimate the hydrogeological properties directly using geoelectrical parameters (Chandra et al. 2008; Sri Niwas and Celik 2012). The analytical equation is developed based on how hydrogeological properties and current flow depend similarly on several factors. Through the developed analytical equation, the geoelectrical parameters are used to determine the hydrogeological properties. Therefore, accurate geoelectrical parameters need to be acquired for estimation purposes. Nevertheless, few studies exist that focus on improving the accuracy of geoelectrical parameters for either the regression or the analytical equation. Furthermore, most of these studies used vertical electrical sounding to acquire the geoelectrical parameters. Therefore, the purpose of this paper is to obtain geoelectrical parameters with higher accuracy by fusing the ER and IP methods to develop the analytical equation.

Methodology

Study area

The study area is located at Universiti Putra Malaysia (UPM), Selangor, Malaysia, with a total area of approximately 21,009 km^2. It lies within the geographical coordinates between 79,000 m and 81,000 m east and 32,000 m and 34,000 m north (UTM zone 47 N). This region was chosen for the hydrophysical study because the geological and hydrogeological characteristics of the area are known. The study area and the distribution of formations are illustrated in Fig. 1. There are three main sedimentary rock formations, namely, the Kajang Formation, Kenny Hill Formation, and Kuala Lumpur Limestone Formation within the study area. The details of the rock formations are shown in Table 1.

Hydrogeological setting

A 54-m-deep borehole was drilled at Ladang 2 UPM and marked at the center of line 1 in Fig. 1. The overburden was composed of silty clay, had a thickness of 9 m, and was underlain by a 27-m schist layer. The Serdang aquifer was found at depth of 36 m and consisted of conglomerate and quartzite, as shown in Fig. 2. To estimate the hydrogeological properties, a pumping test was conducted by UPM staff. Based on the analysis, K and T were determined to be 1.811×10^{-7} m/s and 3.934×10^{-4} m^2/s, respectively. The derivation and drawdown versus time data showed that the Serdang aquifer has double porosity flow, confirming that the aquifer is fissured.

Geoelectrical imaging survey

In this study, geoelectrical imaging surveys were conducted to delineate the subsurface formation. Electrical resistivity tomography was performed first and followed by a time-domain IP technique. The ABEM Lund Imaging system was used for data acquisition in the geoelectrical imaging survey. The system consists of a Terrameter SAS4000, an electrode selector (ES 10-64C), a 12-V DC battery, cables, cable joints, electrodes, jumper cables, measuring tape, a GPS, and peg markers. The electrical resistivity technique was performed by employing 61 electrodes connected to the terrameter with the Wenner-Schlumberger array. The electrodes were positioned with equal spacing (5 m) along the profile. Four multicore cables with equidistant takeout for connecting the electrodes were placed along the profile as shown in Fig. 3. Jumper cables were used to connect the electrodes to the takeout. Based on this setup, data acquisition began when the cables were connected to the terrameter and the battery. The electrode contacts were checked to ensure that the electrodes were in good contact with ground (Soupios et al. 2007). The time-domain IP technique is based on the same principles as electrical resistivity methods and was carried out immediately after the electrical resistivity survey using the same setup and electrode arrangements. The main difference is that the electrical resistivity method

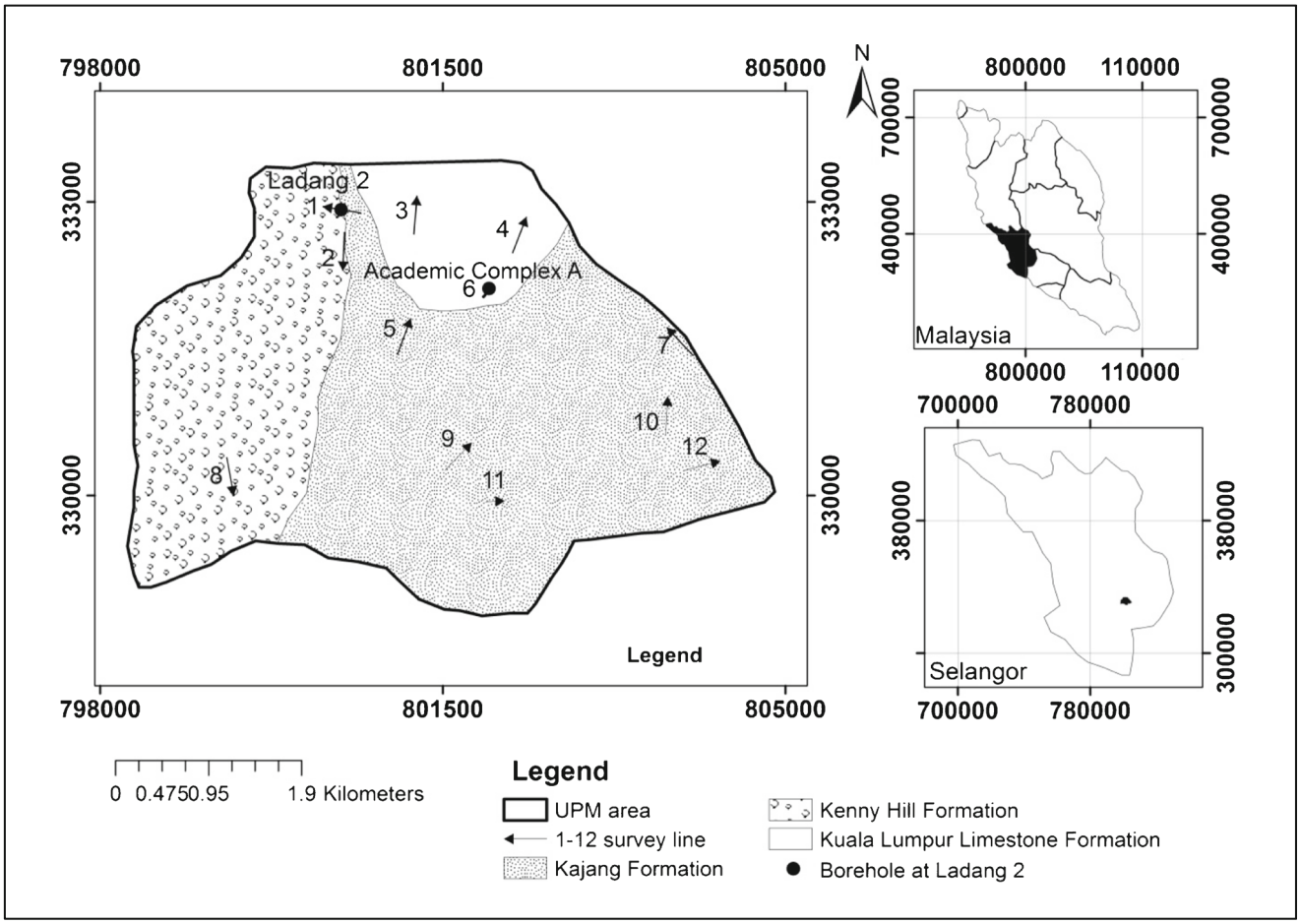

Fig. 1 Study area

used direct current while the IP method injected an alternating current in the form of a square wave. During the IP data acquisition, transient decay of the applied voltage was recorded when the transmitter was switched off. Thus, by integrating the area under the voltage decay curve, the chargeability of the geological formation can be evaluated (Dahlin, Leroux, and Nissen 2002).

Based on the preliminary survey, there were 12 possible locations within UPM suitable for conducting electrical resistivity surveys. The possible locations were first determined by ensuring that the ground was penetrable by electrodes, had a 400-m long free surface area, and was oriented in a straight line. The ER surveys were performed at Ladang 2 (line 1), the Matriculation Complex (line 2), the student quarters (line 3), the Eleventh College (line 4), the football field (line 5), Academic Complex A (line 6), Ladang 16 Lake (line 7), MARDI Lake (line 8), University Agricultural Park (line 9), Ladang 16 cattle field

Table 1 Description of sedimentary rock formations within the study area (Yin 1976)

Formation	Age	Lithology
K.L. Limestone	Between Ordovician to Silurian	Limestone with minor intercalation of phyllite
Kenny Hill	Carboniferous	Quartzite, phyllite and schist with minor intercalation of limestone
Kajang	Between Ordovician to Silurian	Schist with minor intercalations of limestone and phyllite

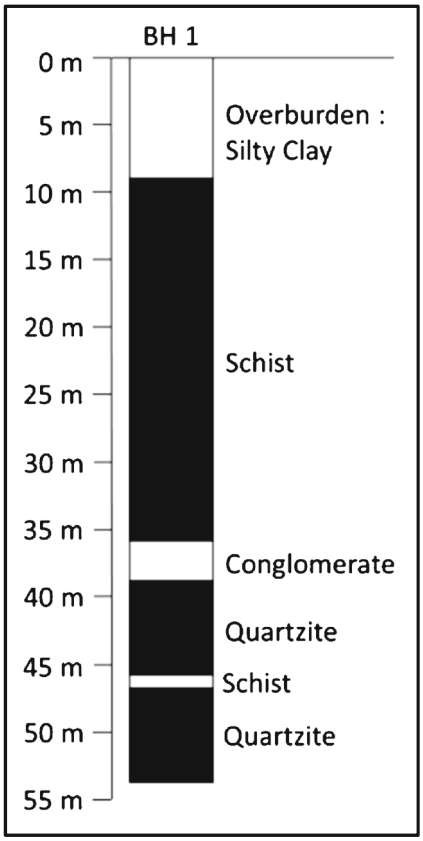

Fig. 2 Borehole lithological log at Ladang 2

(line 10), the University Hospital construction site (line 11), and the Agrobio complex (line 12). The distribution of the survey locations is shown in Fig. 1.

Theoretical development

For a homogeneous fluid like water, hydraulic conductivity depends both on fluid and matrix properties especially porosity. Electric current follows the path of least resistance, as does water. Within and around pores, the mode of conduction of electricity is ionic, and thus, the resistivity of the medium is controlled more by porosity and water conductivity than by the resistivity of the rock matrix. Thus, at the pore level, the electrical path is similar to the hydraulic path and the resistivity should reflect hydraulic conductivity (Niwas and Singhal 1985). Therefore, ′A′ is used as constant of proportionality as shown in Eq. (1).

$$K = A\sigma \;\; or \;\; K = A\frac{1}{\rho} \tag{1}$$

σ, the electrical conductivity, is equal to the reciprocal of the electrical resistivity, ρ. The above relationship indicates that K is proportional to the electrical conductivity, σ, and inversely proportional to the electrical resistivity, ρ. The resistivity is reduced when there is a fracture saturated with groundwater. Then, K is expected to be high. Transmissivity, T, can be obtained by multiplying K with the aquifer thickness, L.

$$KL = A\frac{L}{\rho} \tag{2}$$

or

$$T = AC \tag{3}$$

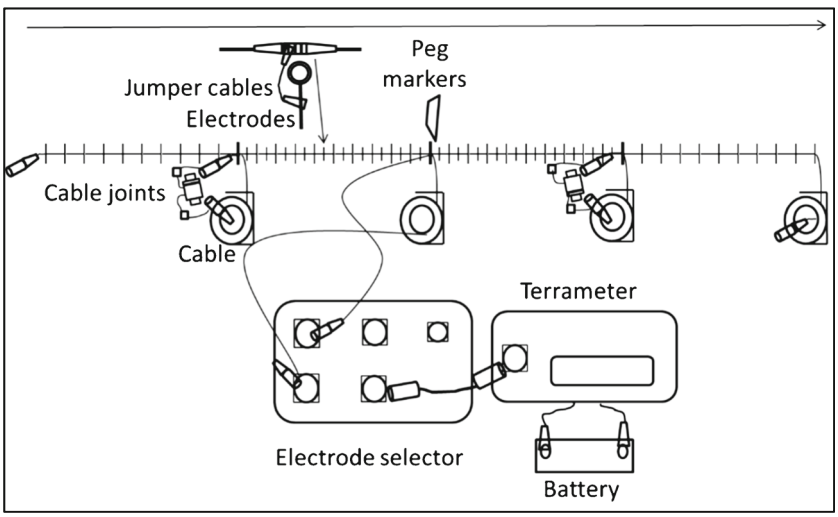

Fig. 3 Geoelectrical imaging survey equipment and arrangement

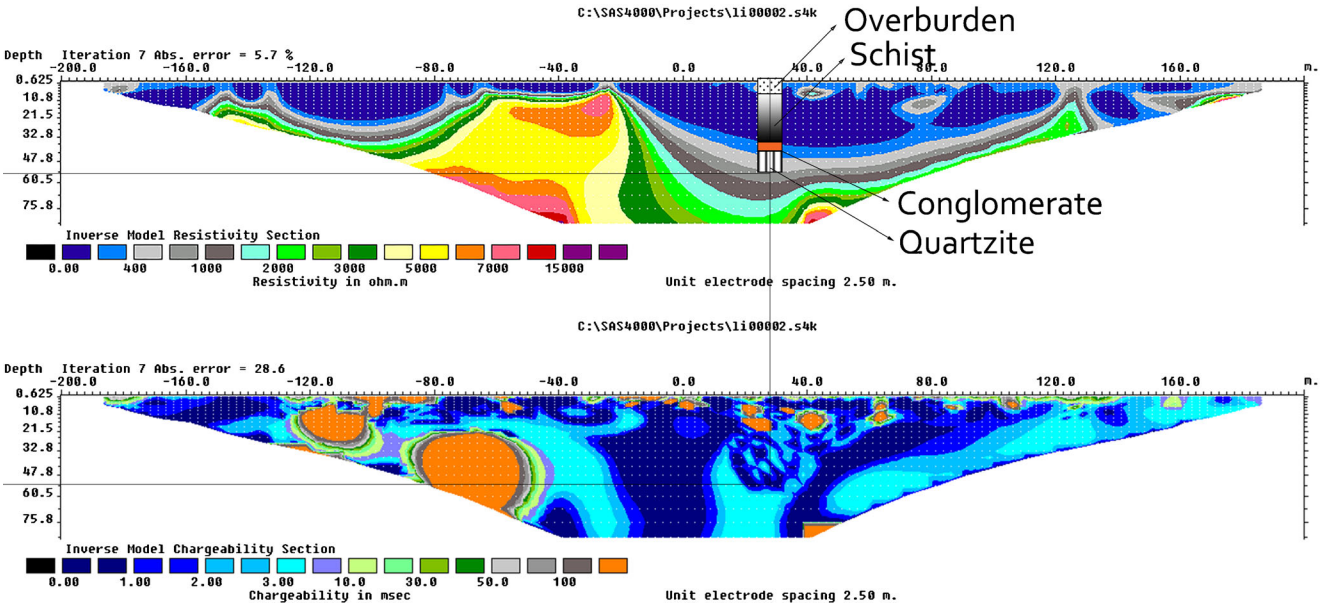

Fig. 4 Tube well at Ladang 2 UPM

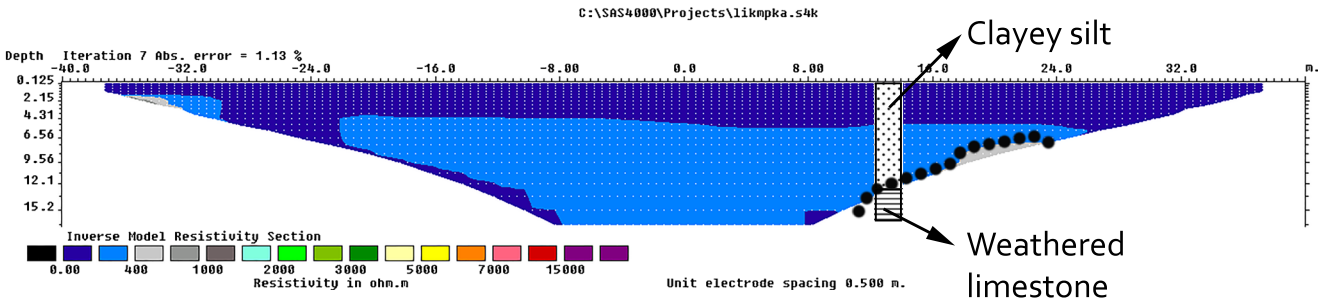

Fig. 5 Borehole at Academic Complex A

where T is the transmissivity (m^2/s) and C is the longitudinal conductance (mho). Since the aquifer thickness is applied in the equations, it is assumed that the fractures/fissures are well connected within the thickness. There is uncertainty in the degree of connection between fractures/fissures. In hard rock, the fracture aperture decreases with depth (Singhal and Gupta 2010). Equations (1) and (3) are valid for well-connected fractures.

Table 2 Resistivity (Keller and Frischknecht 1966) and chargeability values of different materials (Telford et al. 1990)

Material	Resistivity (Ωm)	Material type	Chargeability (msec)
Groundwater (fresh)	10–100	Groundwater	0
Alluvium	10–800	Alluvium	1–4
Sand	60–1000	Gravels	3–9
Clay	1–100	Precambrian volcanics	8–20
Limestone	50–4000	Precambrian gneisses	6–30
Shale	20–2000	Schists	6–30
Sandstone	8–4000	Sandstones	3–12
Granite	5000–1000,000	Argilites	3–10

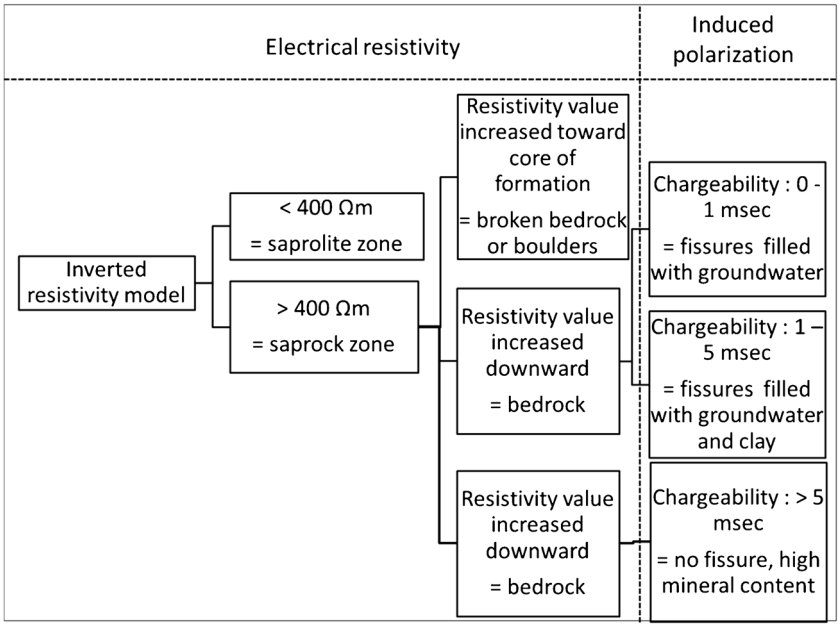

Fig. 6 Delineation of the Serdang aquifer and the fissure content

Results and discussion

Delineation of the Serdang aquifer

The resistivity and chargeability data from the geoelectrical imaging surveys were inverted using RES2DINV to obtain the true 2D resistivity and chargeability image. The geological borehole lithological log information at Ladang 2 and Academic Complex A was used to interpret the geophysical result, as shown in Figs. 4 and 5, respectively. For reference, the resistivity values of different geological materials are shown in Table 2. This study determined ER values of schist, conglomerate, and quartzite ranging from 0 to 200 Ωm, 200 to 400 Ωm, and 400 to 700 Ωm, respectively. Thus, the Kenny Hill Formation had ER values of greater than 400 Ωm. In addition, there was evidence of groundwater within the Ladang 2 borehole at the depth of approximately 36 m b.g.l. with chargeability values ranging from 0 to 4 msec. These

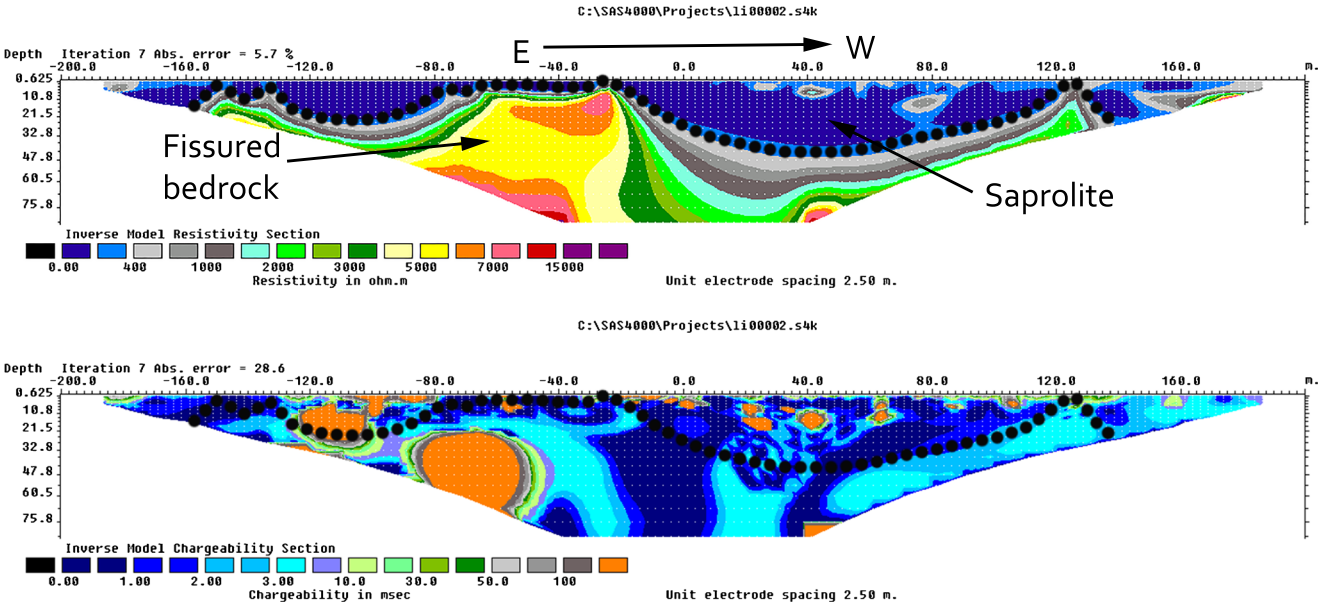

Fig. 7 Fissured bedrock at Ladang 2 (line 1)

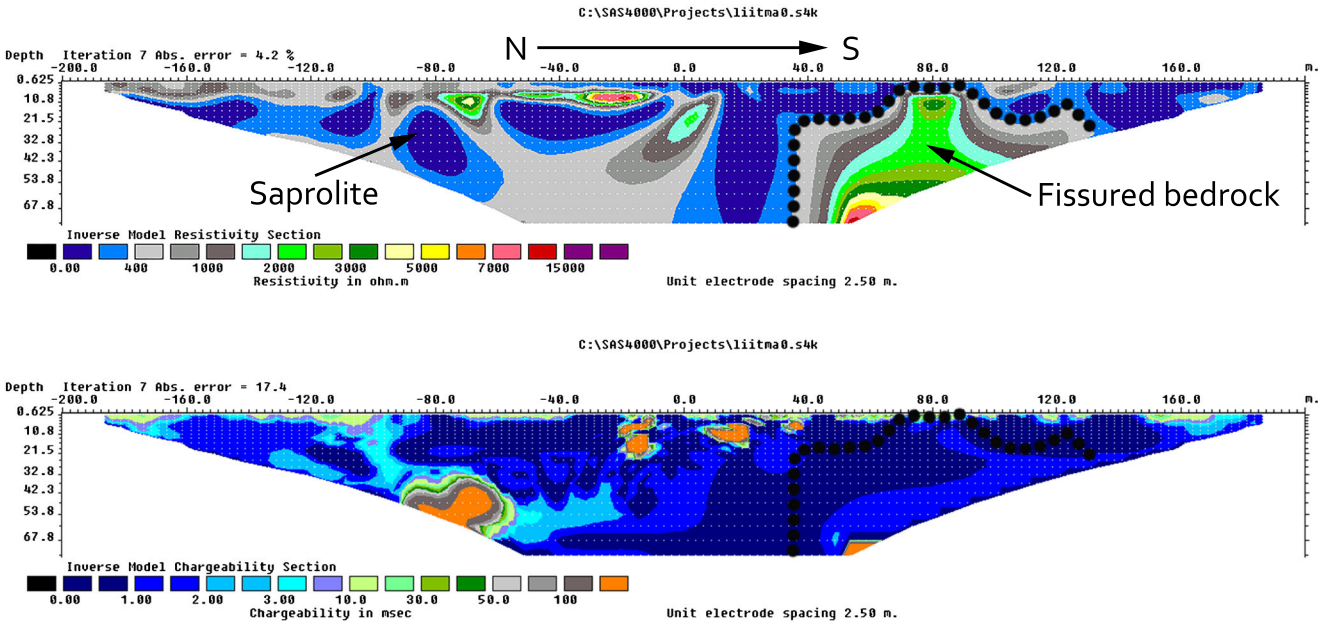

Fig. 8 Fissured bedrock at the Matriculation Complex (line 2)

chargeability values were higher than the values found by other researchers, and the value for pure water should be approximately 0 msec. From the pumping test, it was found that the groundwater contained some clay content that might lead to higher chargeability.

A geophysical method was applied to differentiate between saprock and saprolite. Geological sections with a resistivity value lower than 400 Ωm were classified as saprolite, while other areas were classified as saprock. The upper highly weathered zone was then referred to as saprolite, and the lower broken/fissured zone was referred to as saprock (Comte et al. 2012). In this study, IP was used to identify the groundwater occurrence within the hard rock formation fissures. In general, the chargeability value of groundwater is 0 msec, and according

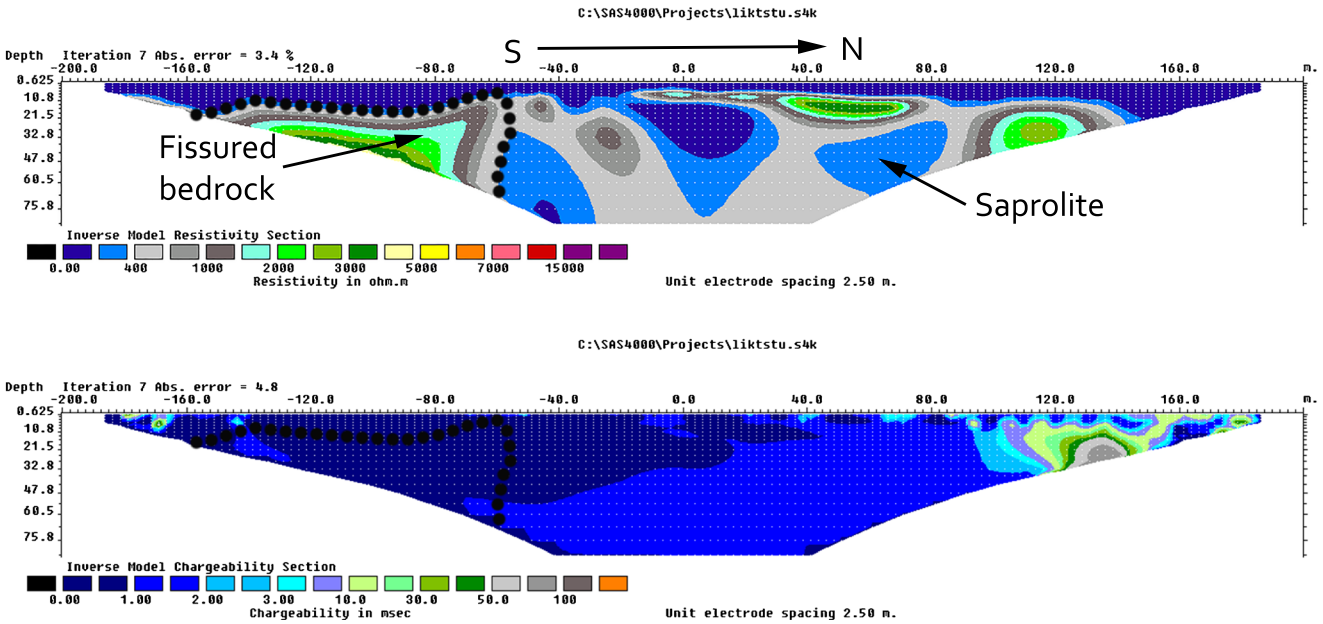

Fig. 9 Fissured bedrock at the student quarters (line 3)

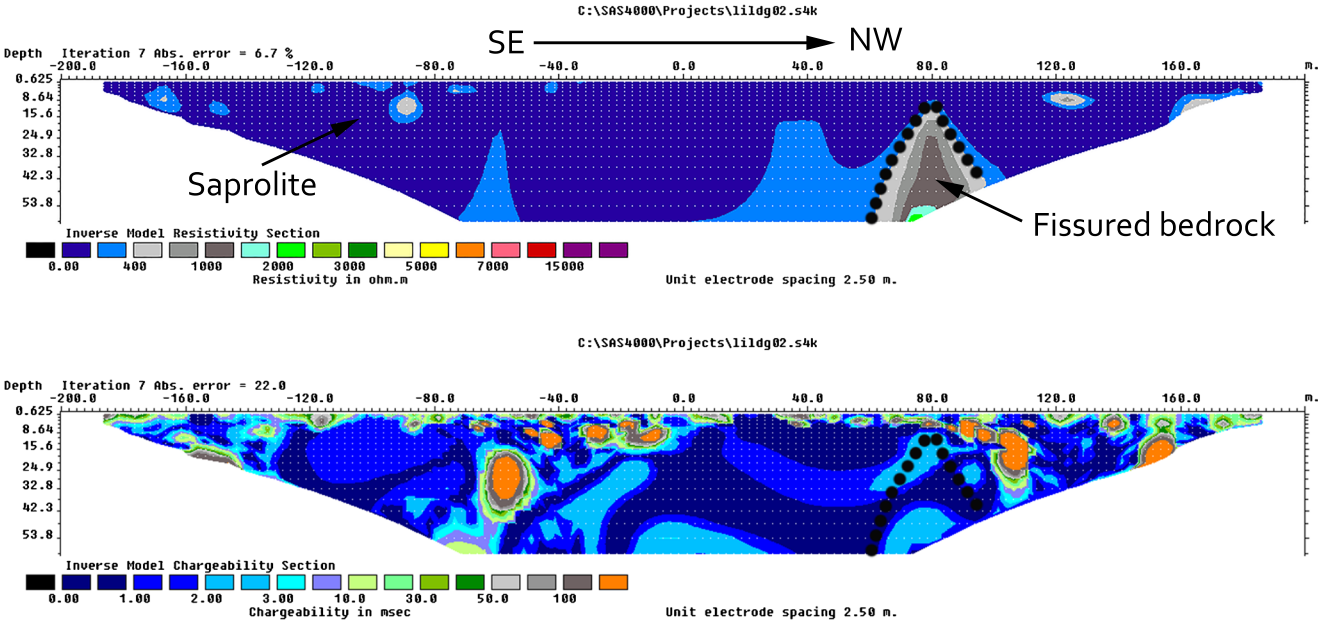

Fig. 10 Fissured bedrock at Ladang 16 Lake (line 7)

to Aristodemou and Thomas-Betts (2000), the chargeability value of clays is below 10 msec. As stated by Aizebeokhai (2014), clays distributed on the surface of grains may have strong IP effects influenced by the clay mineral content.

Through the weathering process, bedrock gradually becomes fissured and finally breaks after a very long time. Within the inverted resistivity image, the resistivity value of bedrock increased downward. Broken bedrock has resistivity values that increase toward the center of the formation, and this bedrock can also become boulders. On the other hand, bedrock that has a chargeability value ranging from 0 to 1 msec may consist of groundwater-containing fissures. Fissured bedrock with chargeability ranging from 1 to 5 msec may contain groundwater (Juanah et al. 2012) mixed with clay, as observed

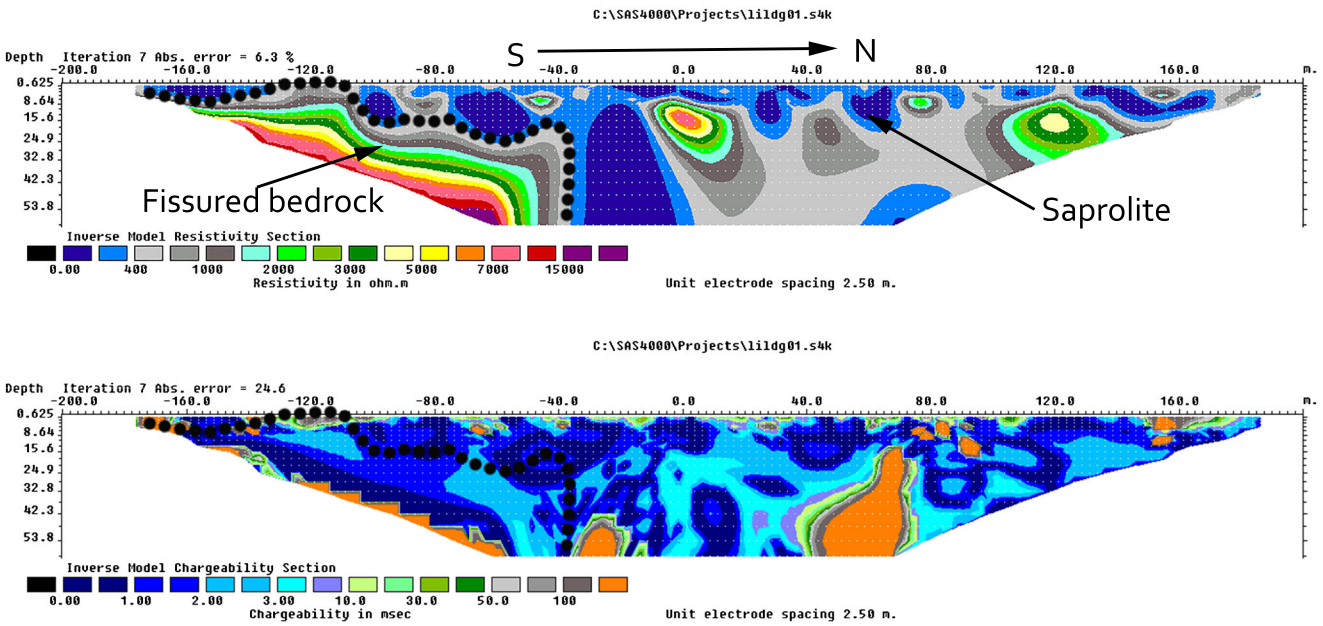

Fig. 11 Fissured bedrock at Ladang 16 cattle field (line 10)

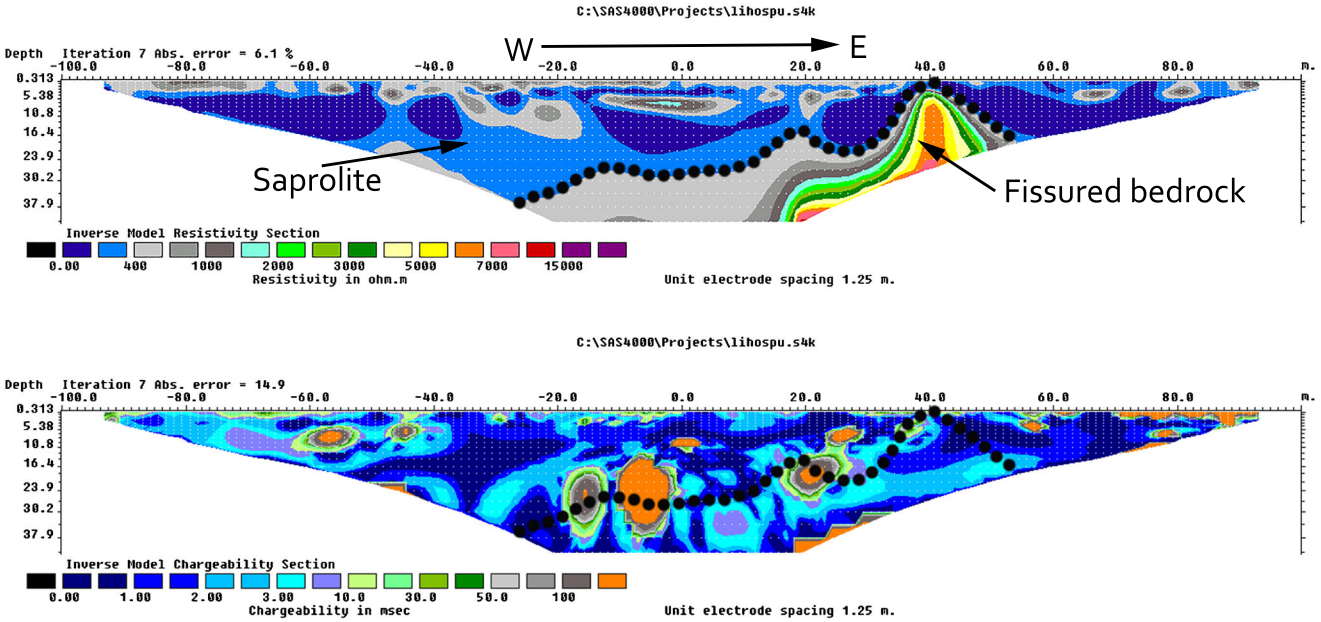

Fig. 12 Fissured bedrock at University Hospital (line 11)

in Ladang 2. Bedrock that has a chargeability above 5 msec may not consist of fissures but have a high mineral content. The classification of the Serdang aquifer and the fissure content is presented in Fig. 6.

This study focused on estimating the hydrogeological properties of fissured bedrock within the Serdang aquifer. Thus, only inverted resistivity and chargeability images of fissured bedrock are shown (Figs. 7, 8, 9, 10, 11, 12, and 13). Dotted lines mark the separation between saprolite and fissured bedrock.

Computation of the electrical resistivity mean

It is crucial to obtain resistivity data points that represent a groundwater conduit within the fissured bedrock. Based on a previous comparison between the borehole lithological log

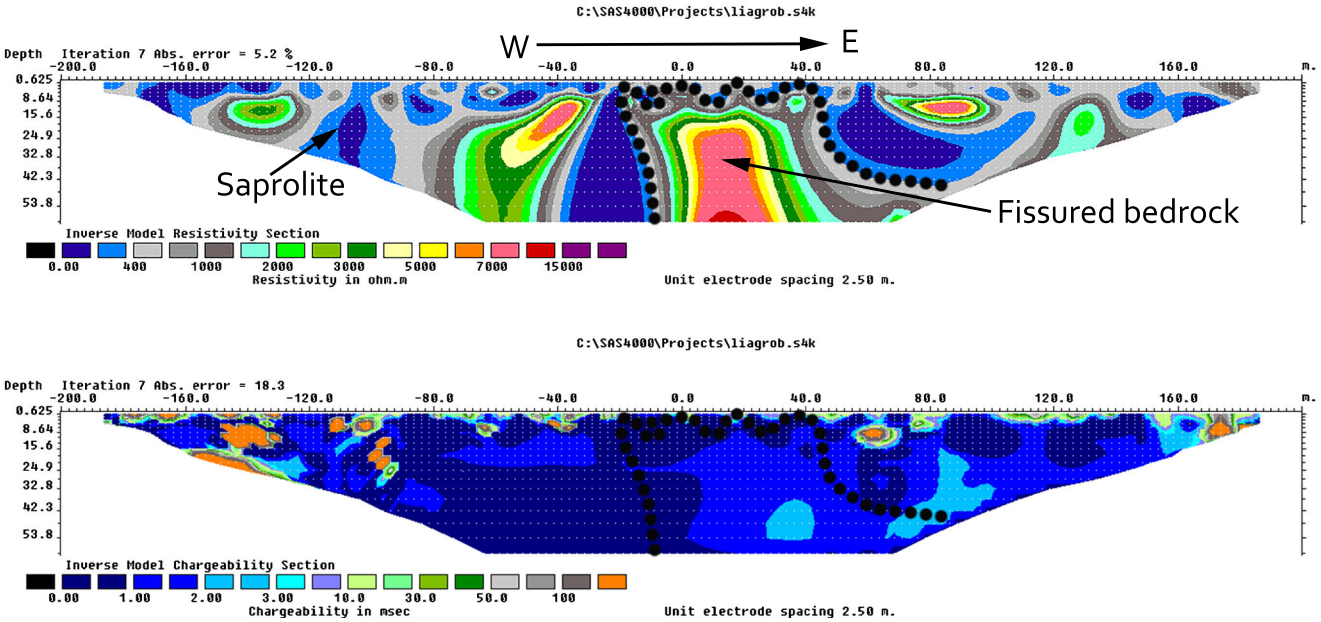

Fig. 13 Fissured bedrock at Agrobio Complex (line 12)

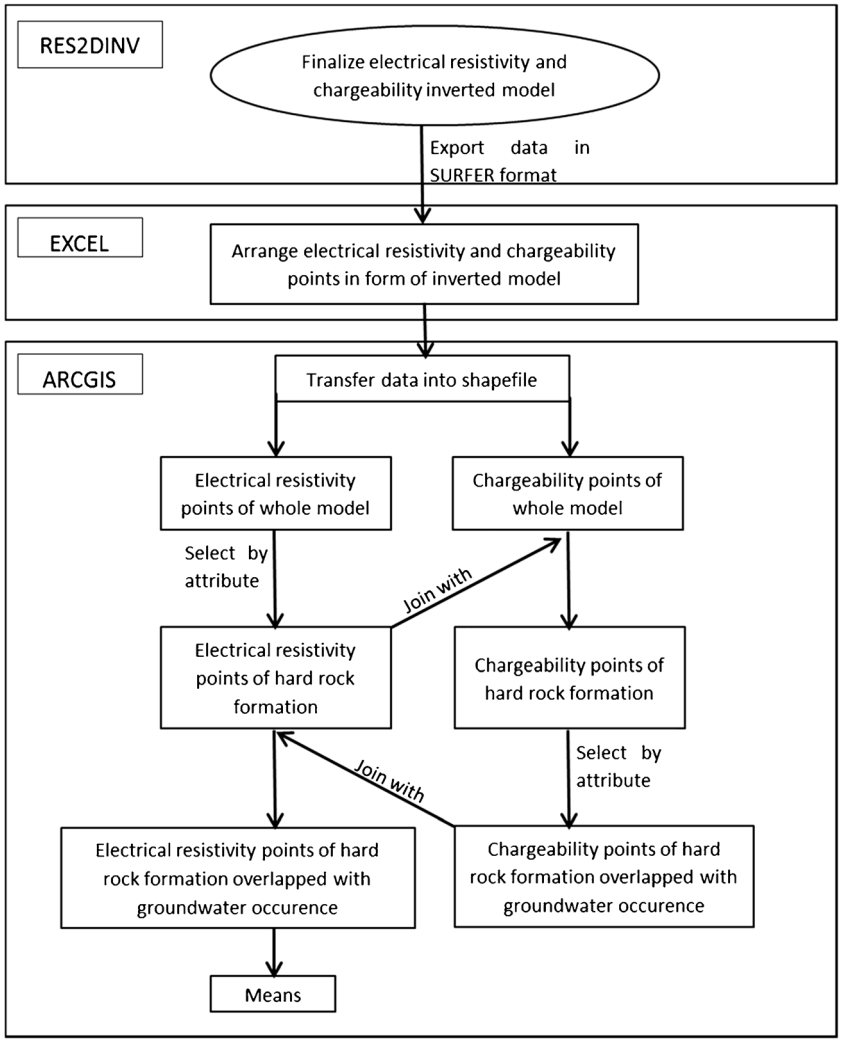

Fig. 14 Workflow to determine means of overlapped electrical resistivity and chargeability points

and the inverted resistivity and chargeability image, it was determined that fissured bedrock containing groundwater has an electrical resistivity greater than 400 Ωm and a chargeability ranging from 1 to 5 msec. Therefore, only electrical resistivity data points greater than 400 Ωm that overlap with chargeability data points ranging from 1 to 5 msec represent a groundwater conduit.

Data points can be selected precisely based on the aforementioned criteria through the assistance of ArcGIS. The values of electrical resistivity and chargeability at each point in the inverted image, as well as the true horizontal length and vertical depth, were stored in a generic file. These data were rearranged in Microsoft Excel before being transferred into ArcGIS and saved in a vector data format known as a shapefile. The workflow is shown in Fig. 14.

First, electrical resistivity data points that represent the fissured bedrock were extracted. Then, chargeability data points that represent groundwater within the fissured bedrock were discretely selected. Some of the electrical resistivity data points overlapped with certain chargeability data points, indicating a potential groundwater conduit, as shown in Fig. 15. Finally, ArcGIS statistics were used to compute the electrical resistivity mean of the overlapping data points.

Measurement of hydrogeological properties

One of the essential requirements for estimating hydrogeological properties from surface geoelectrical measurements is that K from at least one point in the area must be previously known (Sri Niwas and Celik 2012). A pumping test was conducted at the Ladang 2 borehole by UPM staff to obtain the

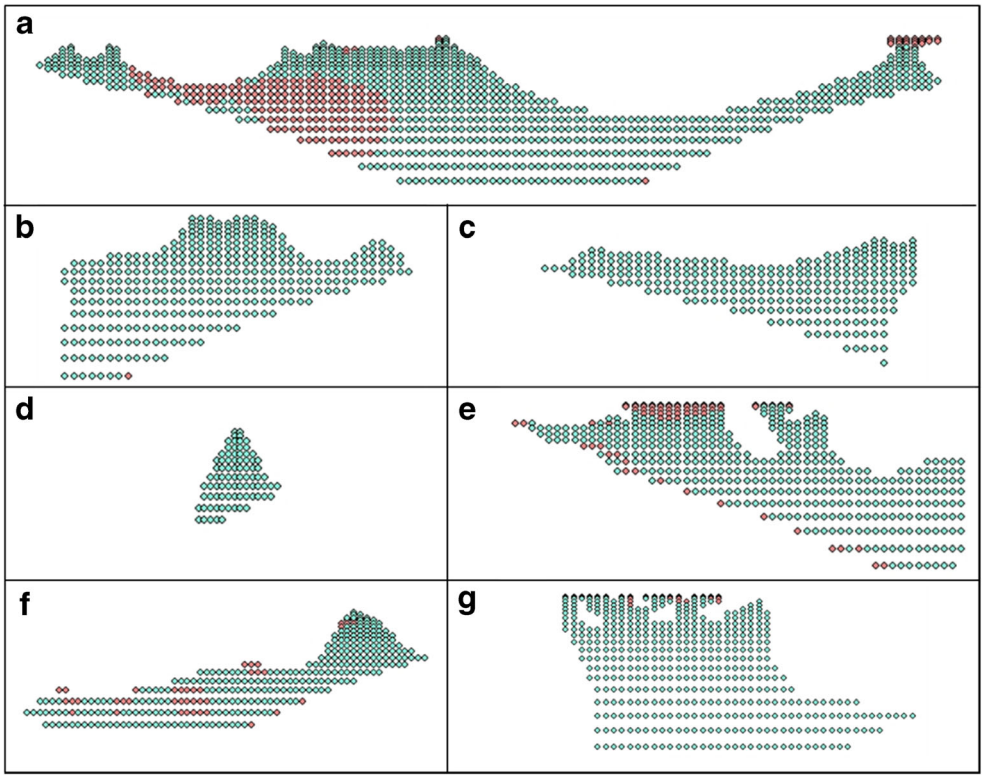

Fig. 15 Blue points indicate the potential groundwater conduit at **a** Ladang 2, **b** Matriculation Complex, **c** Student quarters, **d** Ladang 16 Lake, **e** Ladang 16 cattle field, **f** University Hospital, and **g** Agrobio Complex

hydrogeological properties of the aquifer. A constant discharge pumping test was conducted for 24 h. The drawdown recorded during the pumping test was analyzed using Aquifer Test software, and the hydraulic properties for Ladang 2 are tabulated in Table 3.

According to the analytical equation, the constant '*A*' in Eq. (1) was obtained by multiplying the known *K* at Ladang 2 UPM with the electrical resistivity within the potential groundwater conduit. The *K* values at the other locations were estimated using the constant '*A*' and the electrical resistivity at the respective location using Eq. (1). *T* was estimated using Eq. (3). *T* was computed by multiplying the constant '*A*' with the longitudinal conductance, whereby the aquifer thickness was divided by the average of the electrical resistivity. The average depth of the fissured bedrock's top points was computed using ArcGIS statistics. The aquifer thickness was equal to the difference between the depth of the fissured bedrock's bottom point and the average depth of the fissured bedrock's top point. The computation of *K* and *T* is given in Table 4.

Validating the estimated hydrogeological properties

For validation purposes, the analytical equation was used to estimate the hydraulic properties at Pengerang, Johor, which is

Table 3 Hydraulic properties at Ladang 2 UPM

Location	Constant/ recovery	Property		Average	
Ladang 2 UPM	Constant	T (m^2/s)	7.859×10^{-4}	T (m^2/s)	3.934×10^{-4}
		S	3.350×10^{-4}		
	Recovery	T (m^2/s)	8.507×10^{-7}	S	9.517×10^{-2}
		S	0.19		
		K (m/s) Hvorslev	2.049×10^{-7}	K (m/s)	1.811×10^{-7}
		K (m/s) Bouwer and Rice	1.574×10^{-7}		

Table 4 Estimation of hydraulic properties

No.	Survey location	Aquifer thickness, d (m)	Electrical resistivity average, ρ (Ohm.m)	Hydraulic conductivity, K (m/s)	Constant 'A'	Longitudinal conductance, C = d/ρ	Computed hydraulic conductivity, K_{com} (m/s)	Computed transmissivity, T_{com} (m^2/s)
1	Ladang 2	60.12	2802.77	1.811×10^{-7}	5.077×10^{-4}	0.0128	N/A	N/A
2	Agrobio Complex	42.31	2526.98	N/A	N/A	0.0182	2.009×10^{-7}	9.240×10^{-6}
3	Hospital University	18.25	2012.42	N/A	N/A	0.0070	2.523×10^{-7}	3.554×10^{-6}
4	Ladang 16 Lake	32.42	848.04	N/A	N/A	0.0283	5.986×10^{-7}	1.437×10^{-5}
5	Ladang 16 cattle field	49.45	2511.22	N/A	N/A	0.0111	2.022×10^{-7}	5.635×10^{-6}
6	Matriculation Complex	58.39	1557.36	N/A	N/A	0.0231	3.260×10^{-7}	1.173×10^{-5}
7	Student quarters	67.89	1342.67	N/A	N/A	0.0186	3.781×10^{-7}	9.443×10^{-6}

located 300 km from the study area. Geoelectrical imaging surveys were conducted at Pengerang, Johor, as shown in Fig. 16. Afterward, a tube well was installed at the center of the survey line.

There was a 20-m deep-overburden at the top of Pengerang Well 1. Basalt and granite were found beneath alluvium, as recorded in the borehole lithological log. There was also a 18-m-deep overburden at the top of Pengerang Well 2. Beneath the overburden, there was a thin layer of limestone and a 40-m deep rhyolite layer. The electrical resistivity and chargeability inverted images were compared to the borehole lithological log. The resistivity within the saprock increased downward, corresponding to a classification as bedrock. The chargeability value within the bedrock was between 1 and 5 msec, confirming that the bedrock has fissures and contains groundwater.

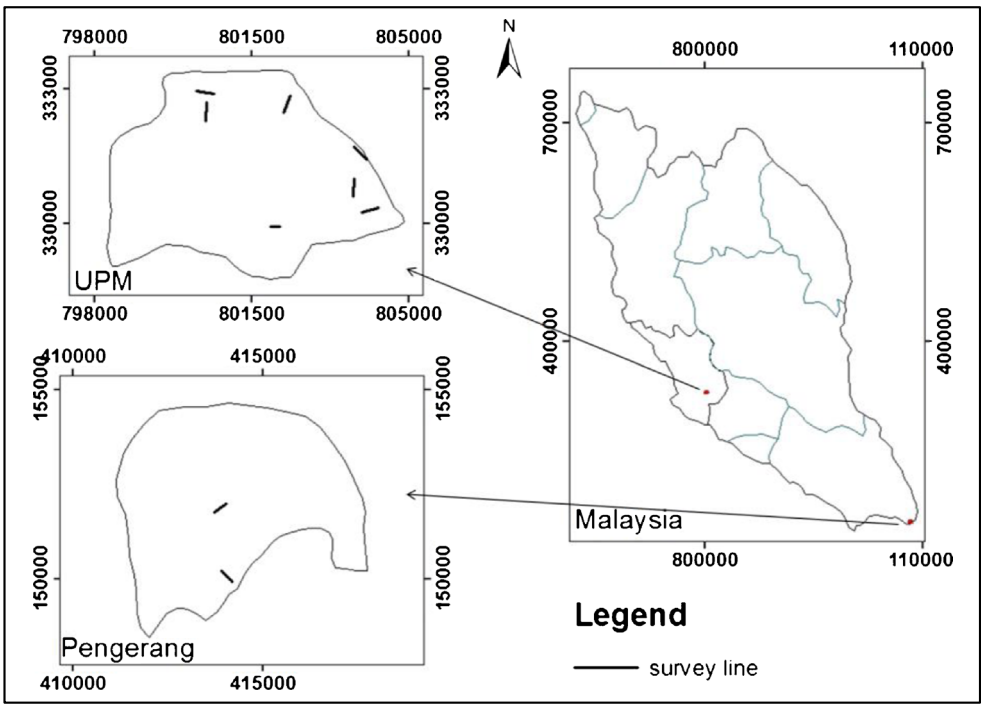

Fig. 16 Geoelectrical imaging surveys at Pengerang, Johor

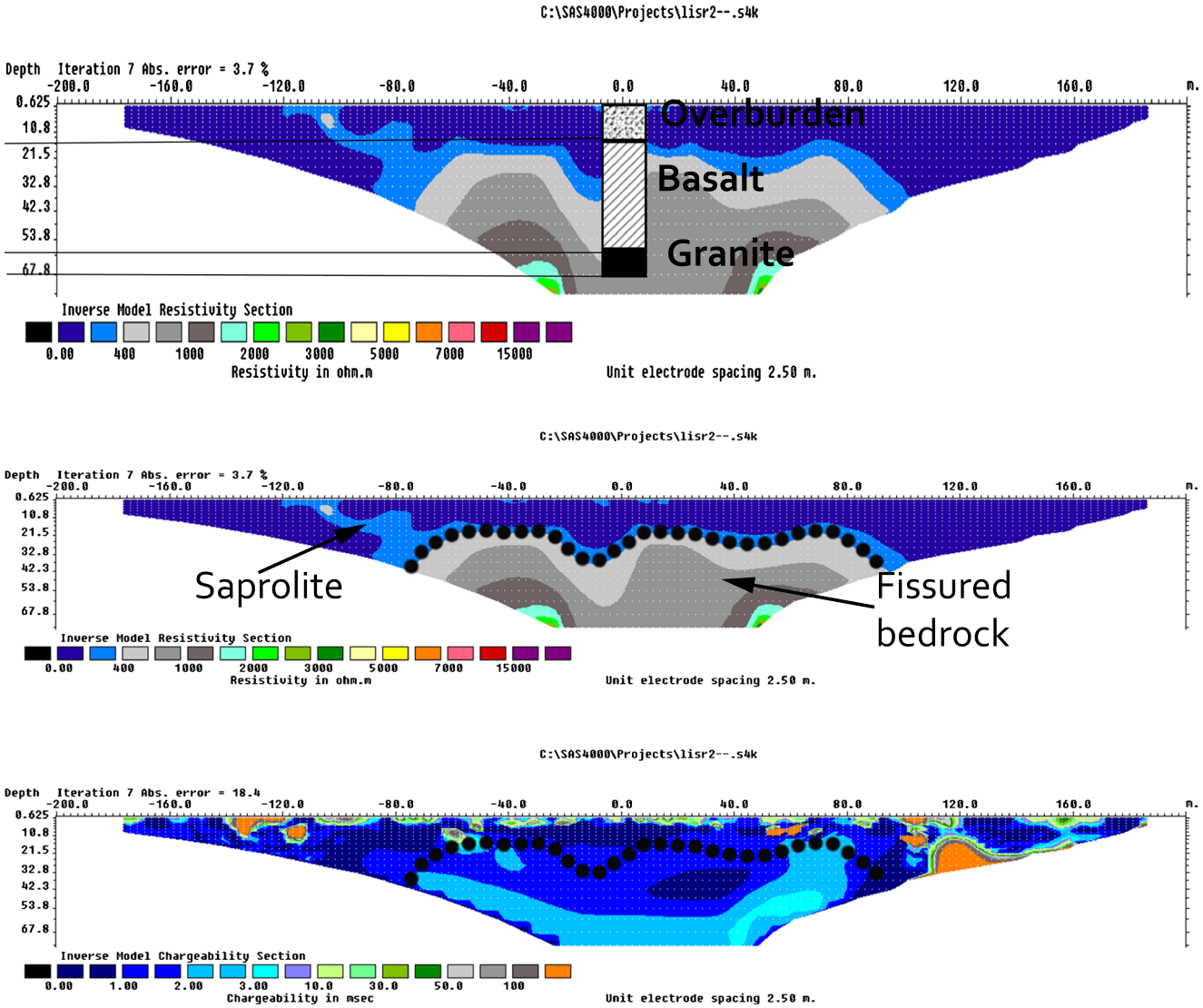

Fig. 17 **a** Comparison between the borehole lithological log at Pengerang Well 1 and the electrical resistivity inverted image. **b** Delineation of fissured bedrock within the inverted resistivity and chargeability images

The delineation of fissured bedrock at Pengerang is shown in Figs. 17 and 18.

A pumping test was conducted to obtain the hydraulic properties of the aquifer. A constant discharge pumping test was conducted for 24 h. The drawdown recorded during the pumping test was analyzed using Aquifer Test Pro software. The hydraulic properties at Pengerang, Johor, are given in Table 5.

The computed K and T values were very similar to the observed K and T values shown in Tables 5 and 6. The mean absolute errors for K and T were equal to 2.846×10^{-7} and 2.291×10^{-5}, respectively, as shown in Table 7. This finding indicates that the analytical equation developed in the study can accurately estimate hydrogeological properties. The aquifer thickness, d, at Ladang 2 and Pengerang was obtained from the borehole lithological log where the pumping test was conducted.

The proposed model was also verified using the Sri Niwas and Celik (2012) and Chandra et al. (2008) studies, which were conducted at an alluvial aquifer and a hard rock aquifer, respectively (Table 8). The values of the constant were calculated based on the relationship "$A = K\rho$" at each point for known values of K. The constant of proposed model in this study, Sri Niwas and Celik (2012) and Chandra et al. (2008) models were computed based on an average of 1, 6, and 11

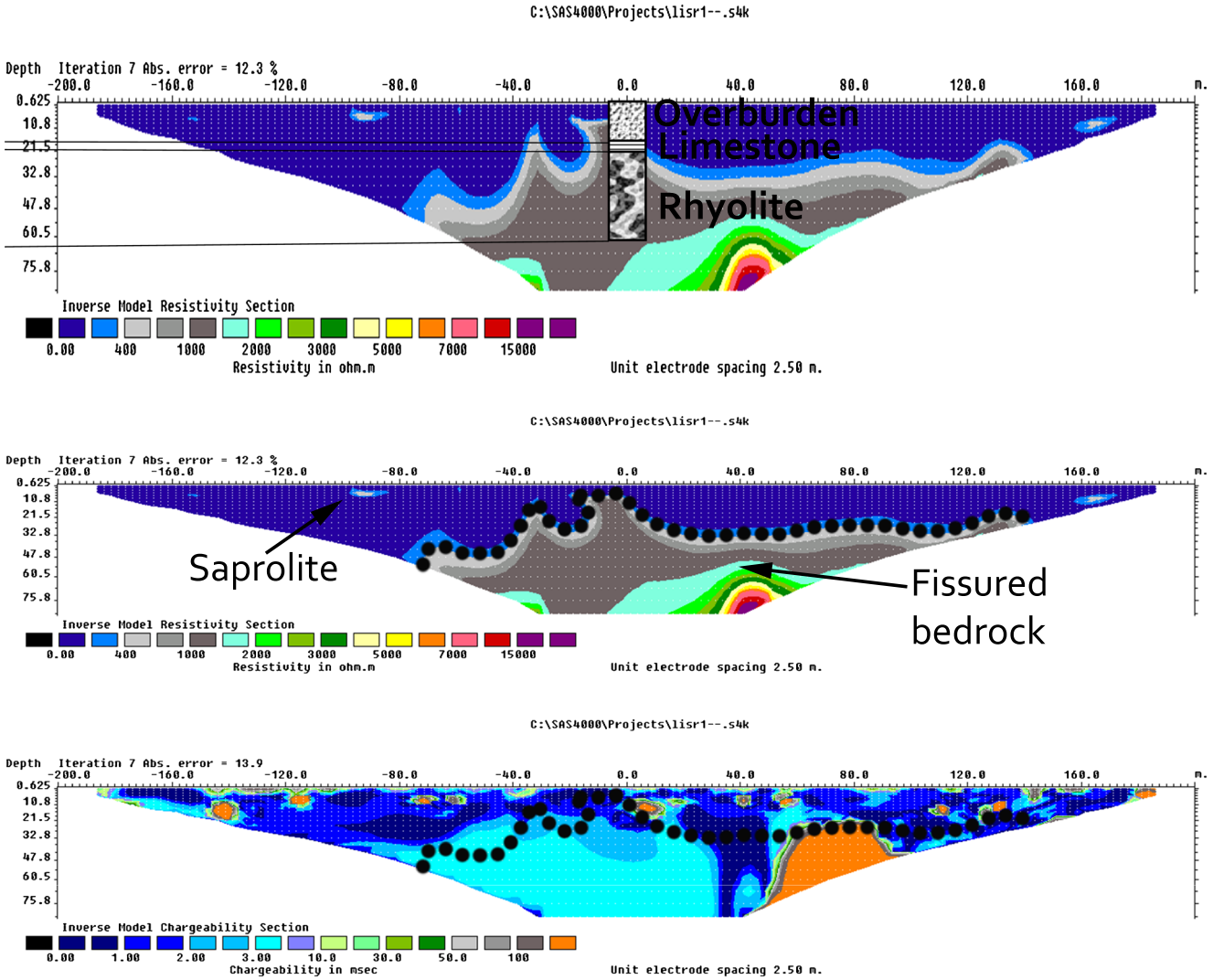

Fig. 18 **a** Comparison between the borehole lithological log at Pengerang Well 2 and the electrical resistivity inverted image. **b** Delineation of fissured bedrock within the inverted resistivity and chargeability images

Table 5 Observed hydraulic properties at Pengerang

Location	Constant/ recovery	Property		Average	
Well 1 Pengerang	Constant	T (m^2/s)	3.218×10^{-5}	T (m^2/s)	1.726×10^{-5}
		S	1.020×10^{-3}		
	Recovery	T (m^2/s)	2.338×10^{-6}	S	0.2505
		S	0.5		
		K (m/s) Hvorslev	2.141×10^{-7}	K (m/s)	1.881×10^{-7}
		K (m/s) Bouwer & Rice	1.620×10^{-7}		
Well 2 Pengerang	Constant	T (m^2/s)	9.826×10^{-5}	T (m^2/s)	5.297×10^{-5}
		S	1.120×10^{-4}		
	Recovery	T (m^2/s)	7.674×10^{-6}	S	0.2501
		S	0.5		
		K (m/s) Hvorslev	5.012×10^{-7}	K (m/s)	4.450×10^{-7}
		K (m/s) Bouwer & Rice	3.889×10^{-7}		

Table 6 Validation of analytical equation at Pengerang

No.	Survey location	Aquifer thickness, d (m)	Electrical resistivity average, ρ (Ohm.m)	Hydraulic conductivity, K (m/s)	Constant 'A'	Longitudinal conductance, C = d/ρ	Computed hydraulic conductivity, K_{com} (m/s)	Computed transmissivity, T_{com} (m^2/s)
1	Ladang 2	60.12	2802.77	1.811×10^{-7}	5.077×10^{-4}			
2	Well 1 Pengerang	47.31	770.81			0.0480	6.586×10^{-7}	2.437×10^{-5}
3	Well 2 Pengerang	53.25	1424.68			0.0281	3.563×10^{-7}	1.427×10^{-5}

Table 7 Absolute error for K and T at Pengerang Wells 1 and 2

Location	Computed K (m/s)	Observed K (m/s)	Absolute error	Computed T (m^2/s)	Observed T (m^2/s)	Absolute error
Well Pengerang 1	6.586×10^{-7}	1.881×10^{-7}	4.705×10^{-7}	2.437×10^{-5}	1.726×10^{-5}	7.110×10^{-6}
Well Pengerang 2	3.563×10^{-7}	4.550×10^{-7}	9.870×10^{-8}	1.427×10^{-5}	5.297×10^{-5}	3.870×10^{-5}
		Mean absolute error	2.846×10^{-7}		Mean absolute error	2.291×10^{-5}

Table 8 Summary of absolute error for K and T by Sri Niwas and Celik (2012), Chandra et al. (2008), and the model proposed by this study

Model	Data from	Average computed K (m/s)	Average observed K (m/s)	Absolute error	Average computed T (m^2/s)	Average observed T (m^2/s)	Absolute error
Sri Niwas et. al	Sri Niwas et. al	2.980×10^{-2}	2.157×10^{-2}	8.234×10^{-3}			
	Chandra	1.205×10^{-1}	2.193×10^{-5}	1.205×10^{-1}	4.037	4.420×10^{-4}	4.037
	Proposed	3.998×10^{-3}	3.166×10^{-7}	3.998×10^{-3}	1.975×10^{-1}	3.511×10^{-5}	1.975×10^{-1}
			Mean absolute error	4.424×10^{-2}	Mean absolute error		2.117
Chandra	Sri Niwas et. al	1.621×10^{-5}	2.157×10^{-2}	2.155×10^{-2}			
	Chandra	6.556×10^{-5}	2.193×10^{-5}	4.363×10^{-5}	2.196×10^{-3}	4.420×10^{-4}	1.754×10^{-3}
	Proposed	2.175×10^{-6}	3.166×10^{-7}	1.859×10^{-6}	1.074×10^{-4}	3.511×10^{-5}	7.233×10^{-5}
			Mean absolute error	7.199×10^{-3}	Mean absolute error		9.133×10^{-4}
Proposed	Sri Niwas et. al	3.782×10^{-6}	2.157×10^{-2}	2.156×10^{-2}			
	Chandra	1.529×10^{-5}	2.193×10^{-5}	6.634×10^{-6}	5.123×10^{-4}	4.420×10^{-4}	7.033×10^{-5}
	Proposed	5.075×10^{-7}	3.166×10^{-7}	1.909×10^{-7}	2.507×10^{-5}	3.511×10^{-5}	1.005×10^{-5}
			Mean absolute error	7.190×10^{-3}	Mean absolute error		2.291×10^{-5}

points of known K values. The proposed model utilized geoelectrical imaging surveys, whereas the other two models applied the vertical electrical sounding (VES) method.

The mean absolute error of the proposed model for K and T was equal to 7.190×10^{-3} and 2.291×10^{-5}, respectively, and was the lowest among those of the other studies. It is interesting to note that the analytical equation that utilized the geoelectrical imaging surveys method can be used to estimate hydrogeological properties from geoelectrical parameters that were obtained through VES. However, this condition is applicable to fissured bedrock aquifer only.

Chandra et al. (2008) and the proposed model produced the highest mean absolute error when verified against Sri Niwas and Celik (2012) data. Similarly, the model of Sri Niwas and Celik (2012) also resulted in the highest mean absolute error when verified against data provided by Chandra et al. (2008). This study found that the constant A in the analytical equation model for fissured bedrock and an alluvial aquifer are very different. It was suggested that the best constant values for hard rock and alluvial aquifers are 5.077×10^{-4} and 4, respectively.

Conclusion

This study set out to estimate the hydrogeological properties at several locations within the study area based on a developed analytical equation. The mathematical formulation was developed to connect hydrogeological properties and geoelectrical parameters. The analytical equation was tested with hydrogeological properties measured from a pumping test at Pengerang, Johor. It was found that the computed K and T at Pengerang were very similar to the measured K and T. For further assessment, the developed analytical equation or proposed model was compared with the results of Sri Niwas and Celik (2012) and Chandra et al. (2008). One of the most significant findings from this study is that the best constant value in the analytical equation for a hard rock aquifer is 5.077×10^{-4}.

The second major finding was that the geoelectrical parameters should be acquired by using a combination of the ER-IP methods, which improves the accuracy of hydrogeological property estimation. Taken together, the findings of this study suggest that the analytical equation developed in this study can be applied to other locations composed of fissured bedrock aquifer. The analytical equation in this study was limited by a constant computed based on only one known hydrogeological property. It is recommended that future research should compute the constant based on more than one known hydrogeological property.

Acknowledgements The authors would like to thank Mr. Hafis Ramli, Nur Hidayu Abu Hassan, Nur Zahanim Muhummad Zahir, and colleagues, including staff at KBP Department who assisted with the data acquisition in the field. The authors thank the anonymous reviewer for their critical review that improved the quality of the paper.

Funding This research is funded through the research grant from Universiti Putra Malaysia, IPS Grant no. 9475500.

References

Aizebeokhai AP (2014) Assessment of soil salinity using electrical resistivity imaging and induced polarization methods. Afr J Agric Res 9(45):3369–3378. https://doi.org/10.5897/AJAR2013.8008

Aristodemou E, Thomas-Betts A (2000) DC resistivity and induced polarisation investigations at a waste disposal site and its environments. J Appl Geophys 44(2–3):275–302. https://doi.org/10.1016/S0926-9851(99)00022-1

Batayneh AT (2009) A Hydrogeophysical model of the relationship between Geoelectric and hydraulic parameters , Central Jordan. J Water Resour Prot 2009(December):400–407. https://doi.org/10.4236/jwarp.2009.1

Batte AG, Barifaijo E, Kiberu JM, Kawule W, Muwanga A, Owor M, Kisekulo J (2010) Correlation of Geoelectric data with aquifer parameters to delineate the groundwater potential of hard rock terrain in Central Uganda. Pure Appl Geophys 167(12):1549–1559. https://doi.org/10.1007/s00024-010-0109-x

Chandra S, Ahmed S, Ram A, Dewandel B (2008) Estimation of hard rock aquifers hydraulic conductivity from geoelectrical measurements: a theoretical development with field application. J Hydrol 357:218–227. https://doi.org/10.1016/j.jhydrol.2008.05.023

Comte JC, Cassidy R, Nitsche J, Ofterdinger U, Pilatova K, Flynn R (2012) The typology of Irish hard-rock aquifers based on integrated hydrogeological and geophysical approach. Hydrogeol J 20:1569–1588. https://doi.org/10.1007/s10040-012-0884-9

Dahlin T, Leroux V, Nissen J (2002) Measuring techniques in induced polarisation imaging. J Appl Geophys 50(3):279–298. https://doi.org/10.1016/S0926-9851(02)00148-9

Farid A, Jadoon K, Akhter G, Iqbal MA (2013) Hydrostratigraphy and hydrogeology of the western part of Maira area, Khyber Pakhtunkhwa, Pakistan: a case study by using electrical resistivity. Environ Monit Assess 185(3):2407–2422. https://doi.org/10.1007/s10661-012-2720-z

Juanah MSE, Ibrahim S, Sulaiman WNA, Latif PA (2012) Groundwater resources assessment using integrated geophysical techniques in the southwestern region of Peninsular Malaysia. Arab J Geosci. https://doi.org/10.1007/s12517-012-0700-9

Keller GV, Frischknecht FC (1966) Electrical methods in geophysical prospecting. Pergamon Press. 523 pp

Khalil MA, Monterio Santos FA (2009) Influence of degree of saturation in the electric resistivity–hydraulic conductivity relationship. Surv Geophys 30(6):601–615. https://doi.org/10.1007/s10712-009-9072-4

Mastrocicco M, Vignoli G, Colombani N, Zeid NA (2009) Surface electrical resistivity tomography and hydrogeological characterization to constrain groundwater flow modeling in an agricultural field site near Ferrara (Italy). Environ Earth Sci 61(2):311–322. https://doi.org/10.1007/s12665-009-0344-6

Niwas S, Celik M (2012) Equation estimation of porosity and hydraulic conductivity of Ruhrtal aquifer in Germany using near surface geophysics. J Appl Geophys 84:77–85. https://doi.org/10.1016/j.jappgeo.2012.06.001

Niwas S, Singhal DC (1985) Aquifer transmissivity of porous media from resistivity data. J Hydrol 82(82):143–153

Perdomo S, Ainchil JE, Kruse E (2014) Hydraulic parameters estimation from well logging resistivity and geoelectrical measurements. J Appl Geophys 105:50–58. https://doi.org/10.1016/j.jappgeo.2014.02.020

Singhal BBS, Gupta RP (2010) Fractures and discontinuities. In: Applied Hydrogeology of Fractured Rocks. Springer, Netherlands. https://doi.org/10.1007/978-90-481-8799-7

Sinha R, Israil M, Singhal DC (2009) A hydrogeophysical model of the relationship between geoelectric and hydraulic parameters of anisotropic aquifers. Hydrogeol J 17(3):495–503. https://doi.org/10.1007/s10040-008-0424-9

Slater L (2007) Near surface electrical characterization of hydraulic conductivity: from Petrophysical properties to aquifer geometries—a review. Surv Geophys 28:169–197. https://doi.org/10.1007/s10712-007-9022-y

Soupios P, Kouli M, Vallianatos F (2007) Estimation of aquifer hydraulic parameters from surficial geophysical methods: a case study of Keritis Basin in Chania (Crete–Greece). J Hydrol 338:122–131. https://doi.org/10.1016/j.jhydrol.2007.02.028

Taheri TA, Voudouris KS, Eini M (2007) Groundwater balance, safe yield and recharge feasibility in a semi-arid environment: a case study from western part of Iran. J Appl Sci 7:2967–2976. https://doi.org/10.3923/jas.2007.2967.2976

Telford WM, Geldart LP, Sherrif RE (1990) Applied geophysics (Second). Cambridge University Press, Cambridge

Utom AU, Odoh BI, Egboka BCE, Egboka NE, Okeke HC (2013) Estimation of subsurface hydrological parameters around Akwuke, Enugu, Nigeria using surface resistivity measurements. J Geophys Eng 10(2):25016. https://doi.org/10.1088/1742-2132/10/2/025016

Yin EH (1976) Geological map of Kuala Lumpur, Selangor. Geological Survey Malaysia, Ipoh, Perak, Malaysia. Sheet No. 94